Micro and Nano Systems Letters

CORRESPONDENCE Open Access

A novel application of the micro-wire-electro-discharge-grinding (μ-WEDG) method for the generation of tantalum and brass nanoparticles

Akash Korgal[1*], P. Navin Karanth[1], Arun Kumar Shettigar[1] and J. Bindu Madhavi[2]

Abstract

The synthesis of a co-precipitated mixture of tantalum and brass nanoparticles (Ta and Cu/Zn) using a micro-wire-electro-discharge-grinding (μ-WEDG) with a combination of multiple process parameters is explained in this article. Tantalum and brass nanoparticles are produced in a dielectric medium Diel-7500 EDM oil. μ-WEDG represents a cutting-edge mechanical micro-machining technique extensively employed for machining micro rods. This method uses a grinding process that expels debris via melting and evaporation. This process disperses a fraction of nanometre-sized debris within the dielectric medium. Traditionally, this debris consisting of nanoparticles has been classified as unwanted substances and subsequently eliminated from the system. However, it now requires a thorough reassessment for possible usage. Hence, the characterization of tantalum and brass nanoparticles is conducted through Field emission Scanning Electron Microscopy (FE-SEM), energy-dispersive spectroscopy (EDS), and X-ray diffraction (XRD) analyses. The process parameters are capacitance, voltage and spindle speed. The investigation reveals that the mean nanoparticle size of produced tantalum nanoparticles range from 25 to 200 nm, while brass nanoparticles range from 300 to 950 nm. Furthermore, a notable correlation is observed between decreasing capacitance and the corresponding reduction in the shape and size of nanoparticles.

Keywords WEDG, Synthesis, Nanoparticles, Tantalum, Cytotoxicity

Introduction

The advent of advanced microfabrication techniques has significantly expanded the horizons of material processing and precision engineering. Among these, Micro-Wire-Electro-Discharge-Grinding (μ-WEDG) has emerged as a pioneering method, enabling the generation of ultra-fine features with exceptional accuracy. A thin, continuous wire serves as the electrode, while the workpiece itself is submerged in a dielectric fluid. Particularized melting and vaporization of the material are caused by sparks produced between the wire and the workpiece, effectively removing it from the desired location. This technique is particularly advantageous for the production of nanoparticles from refractory and non-refractory metals as well. Advancement of micro and nanoscience materials has sparked a fresh wave of enthusiasm among researchers and scientists due to the development of micro and nanoscience technologies. Government and businesses are interested in nanoscience since its potential is becoming more widely recognized. As a result, significant investments are being made in micro and

*Correspondence:
Akash Korgal
akashk.217me001@nitk.edu.in
[1] Department of Mechanical Engineering, National Institute of Technology Karnataka, NH 66, Srinivasnagar, Surathkal, Mangaluru, Karnataka 575025, India
[2] Department of Mechatronics Engineering, Mangalore Institute of Technology and Engineering, Badaga Mijar, Solapur -Mangalore Highway, Near Moodabidre, Mangaluru, Karnataka 57422, India

nanoscale technologies to use their potential and advance numerous sectors [1]. Nanoparticles are crucial in forming nanostructures, serving as the nanoscale building elements. Typically, these particles usually have sizes between 1 and 100 nm. Even at this nanoscale, materials display remarkable physical properties distinct from their bulk counterparts. The material demonstrates a reduced melting point, an elevated surface-to-volume ratio, enhanced mechanical strength, unique optical features, and special magnetic attributes. Researchers emphasise the significance of nanomaterial manufacturing due to its exceptional characteristics, this might be used in several sectors and have a broad variety of uses [2–4]. They have demonstrated their indispensability in material technology for several applications such as ferrofluids [5], chemical nanosensors [6], hydrogen storage [7], catalytic systems [8], and some microelectronics devices. Furthermore, nanoparticles are crucial in the fields of nanomedicine, agriculture, the military, and the energy sector, showcasing their adaptability and significance in shaping contemporary technologies and industries [9]. The distinct capability of metallic nanoparticles to interact with ligands, medicines, and antibodies has generated significant interest. The first studies on non-conventional machining of biomaterials used a common dielectric fluid and yielded significant findings [10].

The μ-EDM approach was used to synthesize and analyse colloidal nanoparticles of aluminium, in the investigation influence of various stabilizers on nanoparticle agglomeration was explored. The base media was deionized water, and, Bael Gum (BG), Poly Ethylene Glycol (PEG), and Acacia Gum (ACG) were each introduced individually to examine their effects on the interactions between the synthesized nanoparticles. ACG exhibited the most significant effect in minimizing agglomeration, leading to an exceptionally uniform distribution of colloidal aluminium nanoparticles [11]. During a research investigation on the production of nanoparticles using μ-EDM, polyvinyl alcohol (PVA) was combined with a dielectric substance in order to stabilize the nickel nanofluid and reduce effects of agglomeration. The characteristics of the produced nickel nanoparticles were assessed by SEM, EDAX EDS, X-ray diffraction (XRD), UV–Vis spectroscopy, and Fourier transform infrared (FTIR) analysis. The study observed a shift in nanoparticle morphology from spherical shapes at higher pulse-on times to needle-like structures at lower pulse-on times [3]. The μ-EDM approach is employed for investigating the synthesis of silver nanoparticles (AgNPs). A variety of dielectric fluids are used to create nanofluids, including non-polar fluids such as kerosene (KR) and ethylene glycol (EG), as well as polar fluids such as deionized water (DI) and deionized water with four weight percent of polyvinyl alcohol (DI + PVA) Kerosene offered the most thermally stable nanofluid with the highest nanoparticle concentration, while DI + PVA resulted in smaller nanoparticles which was observed by Thermogravimetric Analysis (TGA) and Differential Scanning Calorimetry (DSC) [12]. Tungsten carbide nanoparticles were synthesized using μ-EDM in two distinct dielectric mediums, namely kerosene and EDM oil. Subsequently, the rate at which tools deteriorated in each dielectric was examined through the creation of nanoparticles. WC nanoparticle generation and tool wear rate both increased with higher voltage at constant duty factor and EDM oil produced a significantly higher quantity of WC nanoparticles compared to kerosene [13].

The literature review highlights the significant importance of generating nanoparticles of different materials using the μ-EDM technique to meet specific application requirements and efficiently produce nanoparticles for use in science and industry. It can use tiny tools without making contact. μ-EDM is a promising and economical technology due to its simplicity, clean operation, tunability, and lower energy consumption compared to other techniques [14]. μ-WEDG is a revolutionary method that combines nanotechnology and non-traditional grinding processes to produce nanoparticles. Currently, conventional WEDG technology combined with an RC electro discharge circuit makes it simple to build micro-electrode tools with diameters as small as a few micrometres [15].This ground-breaking technique uses the μ-WEDG's inherent micro-machining capabilities to precisely and reliably produce tantalum and brass nanoparticles.

Compared to traditional nanoparticle synthesis techniques, this approach has scalability, efficiency, and environmental friendliness benefits. Tantalum with brass nanoparticles are remarkably adaptable for various applications like biomedical implants, gas sensing, catalyst, electronics, surface coatings, and in some energy storage systems, because any base fluid that has metal oxide nanoparticles added to it has improved thermal conductivity [16]. In this technique nanoparticles are shaped to exact sizes and shapes by using the electrical energy of sparks in a dielectric medium. This combination of μ-WEDG and nanotechnology opens up new vistas for inquiry and invention in nanomaterials and prepares the way for cutting-edge study and commercial applications. Any base fluid that has metal oxide nanoparticles added to it has improved thermal conductivity.

Experimentation method and material

The procedure involves using a 1 mm diameter pure tantalum rod as the workpiece, while the revolving wire electrode is built of 0.25 mm thick brass wire. Tantalum R05200 with a purity of 99.11% was obtained. A

μ-WEDG Setup, as depicted in Fig. 1, utilizes an RC-type pulse generator and a digital AC servo motor system with full-closed feedback control. The arrangement comprises a precision work table for X and Y axis movement, a machining tank filled with DIEL-7500 dielectric fluid, and a Z-motion mechanism. The power source has the capability to deliver voltages ranging from 80 to 130 V and capacitances ranging from 0 to 400 Nano farads.

Table 1 presents the experimental conditions for producing tantalum with brass nanoparticles. Acetone was used to clean the Tantalum workpiece and the bathtub to collect the nanoparticles, removing any organic and inorganic foreign substances that had adhered to the surface. Reverse polarity was used to connect the workpiece to the + *ve* terminal and the wire electrode to the − *ve* terminal of the DC pulse supply.

A plasma channel is formed between these electrodes when a significant potential difference causes discharges. A small quantity of material from both electrode and wire melts and evaporates due to this discharge. Key parameters under consideration for this experiment is the inter-electrode gap voltage, capacitance, and the rotational speed of the shaft. During the investigation, spark occurred when the two electrodes were brought closer together within the dielectric medium while applying a specific threshold voltage. The heat produced is limited to a small region and is more significant than the material's melting temperature for both the tools and the workpiece. Consequently, this extreme heat leads to the melting and vaporization of the tools and workpiece material, producing tiny solid particles known as debris.

Table 1 Experimental operating parameters

Sl No	Capacitance in nF	Voltage in V	Spindle speed in rpm
1	400	120	800
2	100	110	800
3	10	100	800
4	1	90	800

These tantalum and brass debris particles are suspended within the dielectric medium, creating a tantalum with brass Nanofluid. This fluid is subsequently collected in glass vials for further analysis and experimentation.

In order to avoid the agglomeration effect, which can occur during production, nanofluid is placed in an ultrasonic bath for six hours. These methods encompass ultrasonication, electrostatic stabilization, and the utilization of stabilizers to mitigate nanoparticle agglomeration. Specifically, ultrasonication is employed

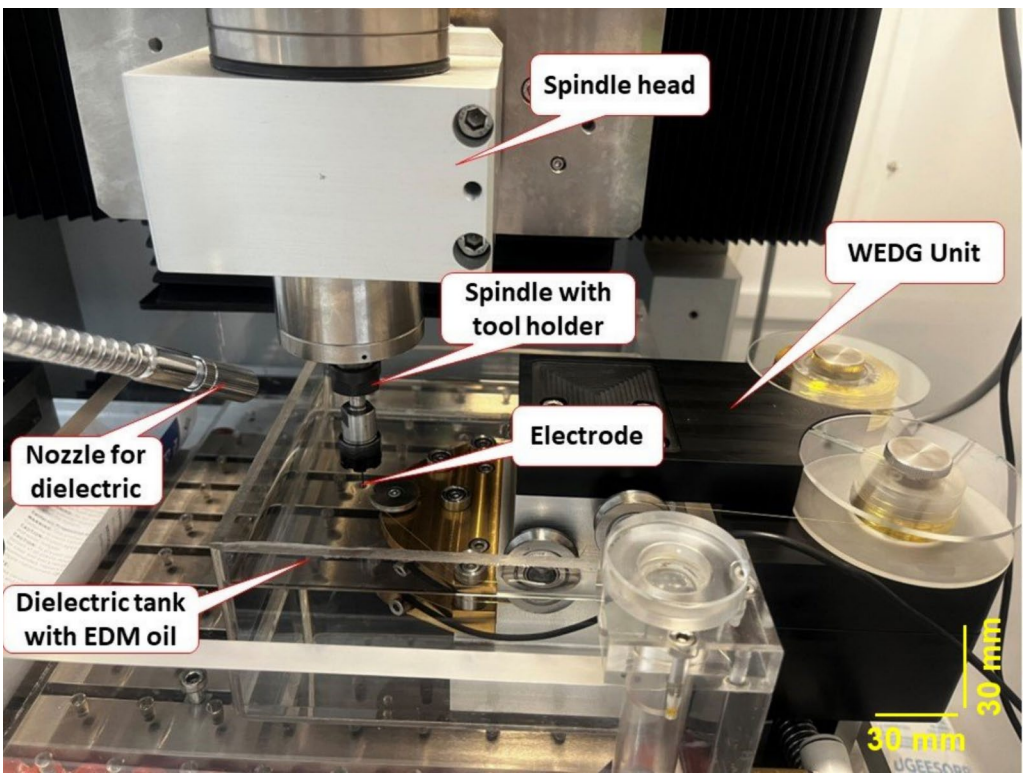

Fig. 1 μ-WEDG setup

to disperse agglomerated nanoparticles within a solvent. Specifically, ultrasonication is employed to disperse agglomerated nanoparticles within a solvent. In the case of achieving a stable tantalum and brass nanofluid, ultrasonication is conducted for 45 min. Subsequently, six washes are performed on the particle solution: three with distilled water and three with ethyl alcohol. At 12,000 rpm, the solution is centrifuged to separate it. Nanoparticles moved throughout this centrifugation process due to the centrifugal force's impact on terminal settling velocity (Vg). Equation (1) shows the link between the unknown settling velocity(V), angular velocity of the centrifuge rotor(w), the radial distance from the centre of rotation(r) under gravitational and centrifugal forces [17].

$$V = \frac{w^2 r}{g} V_g \tag{1}$$

The detailed procedure of extracting synthesized nanoparticles using novel wire electro-discharge grinding is shown in Fig. 2. The obtained nanofluid is then dried for 24 h at 70 °C in an oven.

Characterization of Ta-Cu-Zn Np's

The synthesized tantalum and brass nanoparticles are comprehensively characterized using X-ray diffraction (XRD), field emission scanning electron microscopy (FE-SEM), and zeta potential analysis to gain insights into their morphology, crystal structure, and surface charge. FE-SEM micrographs revealed the morphology and size distribution of the nanoparticles, allowing for estimations of average particle size and identification of any agglomeration tendencies. XRD analysis provided information on the crystal structure of the nanoparticles, confirming the phases present and identifying any potential impurities or amorphous phases. Zeta potential with particle size distribution assessed the nanoparticles' surface charge and average size, which is crucial for understanding their stability and potential interactions with other materials.

These nanoparticles are used in thin film coatings for dental implants. Such coatings promise to enhance biocompatibility significantly, fostering improved integration with surrounding bone tissue and potentially reducing the risk of rejection and inflammation. Additionally, these coatings could offer superior wear resistance, creating a harder, more durable surface that extends the implant's lifespan and minimizes wear over time.

Chemical and regents

Before incorporating the synthesized nanoparticles into dental implant coatings, their cytotoxicity are evaluated using the MTT assay. Trypsin–EDTA solution (catalogue number TCL155) and Antibiotic Antimycotic Solution, Penicillin & Streptomycin (catalogue number A001A) are purchased from Himedia to manipulate cells. Camptothecin is procured from Sigma Aldrich, India (catalogue number C9911) for specific treatments.

Cell culture and Ta-Cu-Zn NP's exposure

This study utilized the Human Dental Pulp Fibroblast Cell Line sourced from NCCS, Pune, India. The cell culture is facilitated by DMEM-F12 media and Fetal Bovine Serum obtained from Himedia (catalogue numbers AL140 and

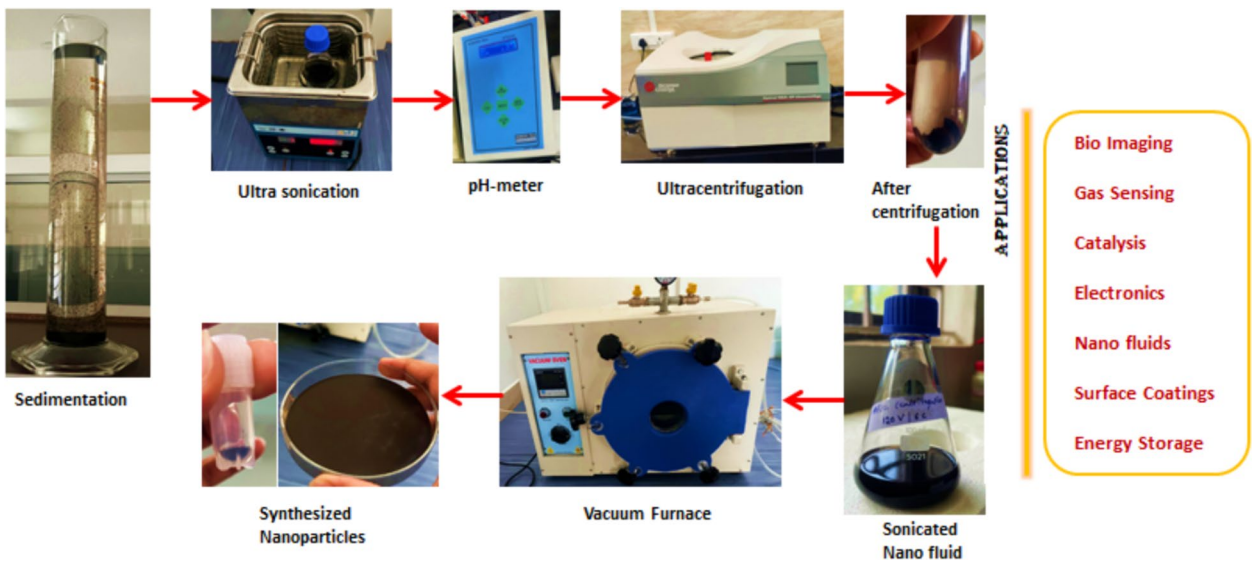

Fig. 2 Procedures for extracting synthesized Nanoparticles

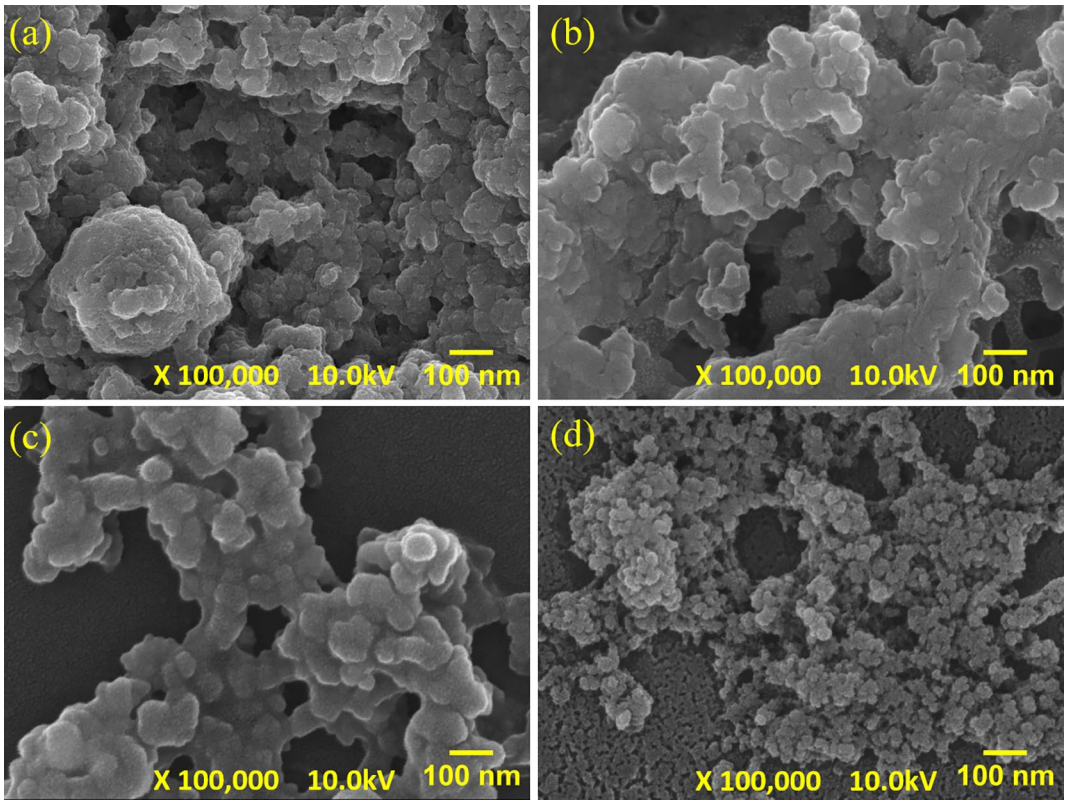

Fig. 3 FE-SEM images of Ta-Cu-Zn Nano particles in EDM oil at **a** 120V & 6C, **b** 110V & 5C, **c** 100V & 4C, **d** 90V & 3C

RM10432, respectively). Additionally, Himedia supplied D-PBS (catalogue number TL1006) for buffer solutions. In a 96-well plate, adherent cells are planted and left to develop overnight. Following that, matching wells are supplemented with different amounts of nanoparticles, whilst control wells alone received culture media. All plates are incubated for 72 h under standard conditions. The spent medium is removed after incubation, and the MTT assay is performed. By measuring the absorbance of formazan crystals, cell viability was determined relative to controls. Finally, the IC50 value, representing the nanoparticle concentration causing 50% cell death, was derived from a linear logarithmic shown in Eq. 2. This approach enabled a comprehensive assessment of nanoparticle cytotoxicity, informing their potential safety for dental implant applications.

$$Y = Mln(x) + CY \tag{2}$$

Here, Y = 50, M and C are from Graph.

Results and discussion

A comprehensive investigation is performed on the colloidal solution containing the tantalum and brass particles to determine their shape, size morphology, chemical composition, and crystal properties.

FE-SEM analysis

Field Emission Scanning Electron Microscopy (FE-SEM) model 7610FPLUS from Jeol, Japan, is used to examine the size and shape morphology of produced nanoparticles. To prepare samples for analysis, they are affixed to stubs using carbon tape and placed within the FE-SEM sample chamber. The synthesized nanoparticles are shown in FE-SEM images in Fig. 3 at various voltage and capacitance values. These FE-SEM images reveal the characteristic morphology of tantalum and brass nanoparticles. The generated nanoparticles exhibited an almost spherical shape when considered individually. However, due to the agglomeration effect observed under all parametric conditions, this spherical nature may not be evident in the FE-SEM images. However, as voltage and capacitance decreased, there was a gradual reduction in particle size. The FE-SEM images confirm that the size of the particles changed according to the variations in the experimental circumstances, which is consistent with the crystal size determined by XRD analysis. The capacitance value was pivotal in material removal via the wire electrode and workpiece. Higher capacitance values corresponded to increased energy input, resulting in larger spark sizes. As a result, more material melted and evaporated off the surfaces of the tools and workpiece,

Table 2 Average size of tantalum and brass nanoparticles in nm

Sl No	Voltage in V	Capacitance in nF	The average particle size of tantalum in nm	The average particle size of brass in nm	Material removed in mm
1	120	400	150–200	800–950	0.855–0.755
2	110	100	50–70	600–850	0.755–0.655
3	100	10	40–65	400–550	0.655–0.555
4	90	1	25–35	300–450	0.555–0.455

resulting in molten met pool in microns, which caused solidification and the production of nanoparticles.

As capacitance values decreased, the overall volume of the molten pool decreased, resulting in smaller particle sizes as shown in Table 2. In simpler terms, lower capacitance values correlated with smaller generated particle sizes. Figure 3a–d showcases the surface morphology of these particles. Notably, both Ta and Brass components appear spherical and exhibit agglomeration, suggesting they cluster together. The smallest particles are observed under 90 voltage and 3 capacitance conditions, as depicted in Fig. 3d.

The composition of the particle sample is confirmed by EDS (Energy Dispersive X-ray Spectroscopy) examination. Figure 4 showcases the EDS plot, which provides insights of elemental composition of the generated nanoparticles. Notably, tantalum and brass are the primary element present in higher proportions. Nevertheless, the EDS plot also reveals the presence of supplementary elements, including carbon (C) and silicon (Si). This observation can be attributed to the nanoparticles attached to carbon tape and deposited onto silica glass before the EDS examination.

XRD analysis

XRD data were acquired, with diffracted X-ray intensities (I) plotted against 2θ angles as shown in Fig. 5. The EDS spectrum verifies the primary constituents found in the nanoparticles. The synthesized powders exhibit luminous Ta particles that dominate most of the volume. The XRD pattern of the synthesized powders exhibits a prominent peak corresponding to TaC. At the same time, a small peak corresponding to Brass (Cu Zn) is also observed (Fig. 5). The XRD examination of the nanoparticles confirms the presence of TaC(Reference code: 01-071-4792), Ta4C3(Reference code: 00-047-1289), and Cu4Zn8(Reference code: 01-076-3507) phases. It is evident from the XRD plots that the peaks are well-defined and sharp, indicating the Nano crystalline nature of the powder particles. The crystal plane and reflection peak positions remained consistent across all four samples. Furthermore, it was observed that the intensity of these peaks increased as the capacitance value decreased.

In the composition of nanoparticles, zinc (Zn) atoms exhibit a specific structural arrangement. These Zn atoms may undergo doping interactions with tantalum

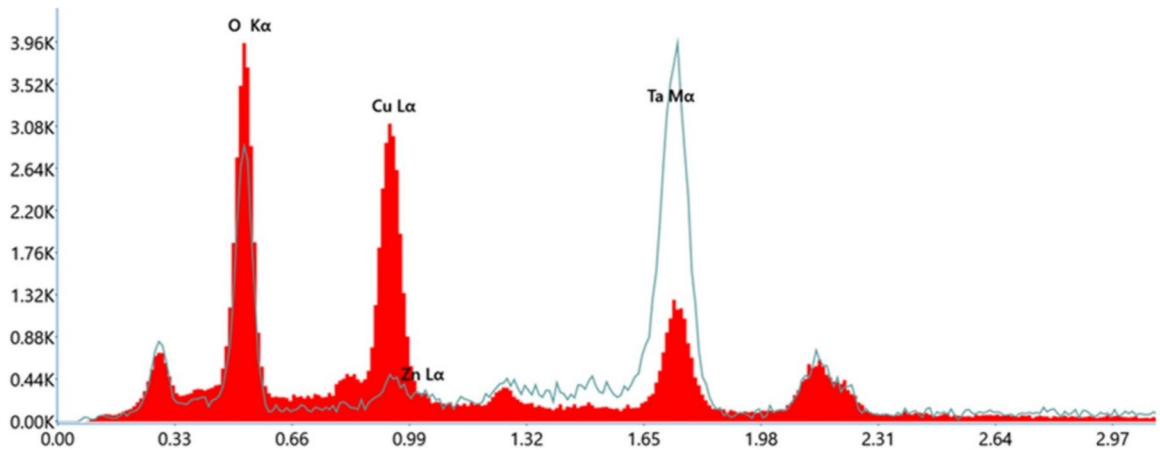

Fig. 4 EDS Result of tantalum and brass nanoparticles

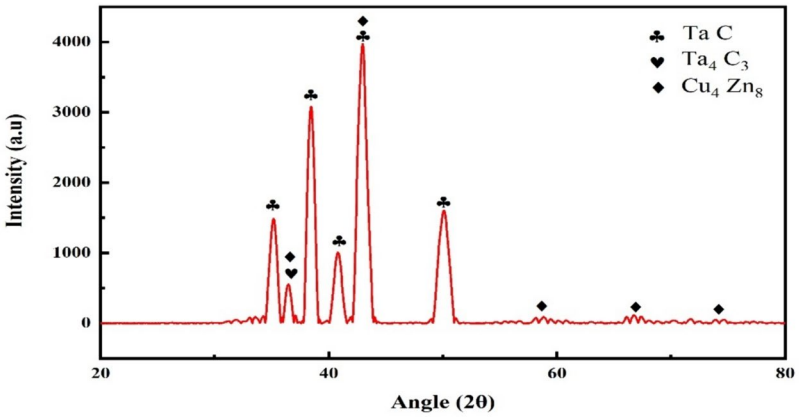

Fig. 5 XRD Result of tantalum and brass nanoparticles

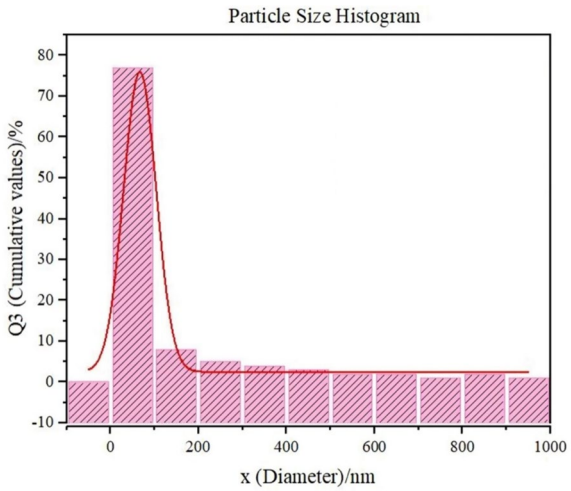

Fig. 6 Distribution of particle sizes of nanoparticles

(Ta) atoms, potentially substituting Ta atoms for Zn atoms. This substitution could result in additional phases, as evidenced by variations in peak positions. The observed shifts in peak positions in the XRD analysis suggest forming distinct crystalline structures, highlighting the complex interplay between Zn and Ta in the nanoparticle composition.

A particle size distribution histogram is shown in Fig. 6. Represents the variation in size of particles within a sample. The x axis represents the particle size in nm and y axis represents the volume percentage of particles within a specific size range. Series of bars on the histogram represents a size range on the x-axis. The height of each bar corresponds to the number or volume percentage of particles that fall within that particular size range. Analysis revealed an average particle size of approximately 975 nm for the synthesized tantalum and brass nanoparticles Fig. 6.

Effects of Ta-Cu-Zn Np's on human dental pulp fibroblast viability

This study evaluated the cytotoxicity of tantalum and brass nanoparticles (Nps) on Human Dental Pulp Fibroblast (HDPF) cell lines. Cells were treated with varying concentrations of the NPs (20, 30, 40, and 50 µM/ml) for 72 h, with an untreated control group serving as the reference (100% viability). The results in Fig. 7 showcased a concentration-dependent decrease in cell viability. As the Np concentration increased, cell viability progressively declined.

Figure 8 Shows HDPF cells in different concentrations where (a) is the untreated cells which appear mostly elongated and spindle-shaped, which is a characteristic morphology of healthy fibroblasts. The cells exhibit a flattened appearance, indicating good attachment to the culture surface. Images (b, c, d and e) Treated with Different Concentrations (20, 30, 40, and 50 µM/ml respectively) appears to be a change in cell morphology across the treated groups (B-E). The cells seem less elongated and more rounded in the treated groups, suggesting a potential effect of the test substance on the cellular cytoskeleton, which is responsible for cell shape and movement. In some treated groups (especially D and E, corresponding to higher concentrations), there are signs of cellular stress. This is indicated by the presence of more round and detached cells, which could be due to factors like reduced cell adhesion or viability.

Overall, these images suggest that the test substance has a concentration-dependent effect on the morphology of HDPF cells. As the concentration increases, the cells become more rounded and detached, indicating potential cytotoxicity.

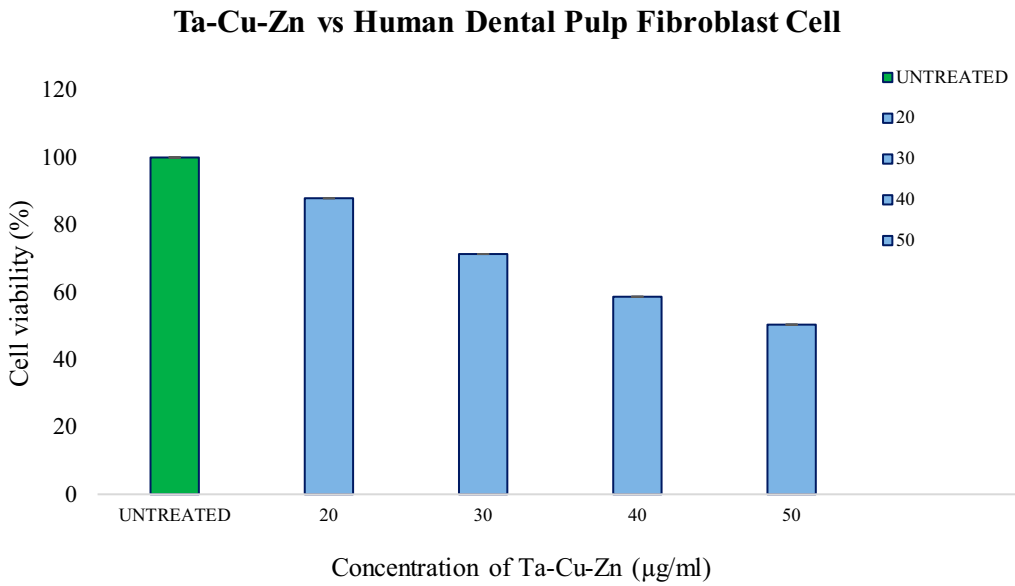

Fig. 7 Mean % cell viability of Human Dental Pulp Fibroblast cell line after exposure to test compound (Ta-Cu-Zn) for 72h

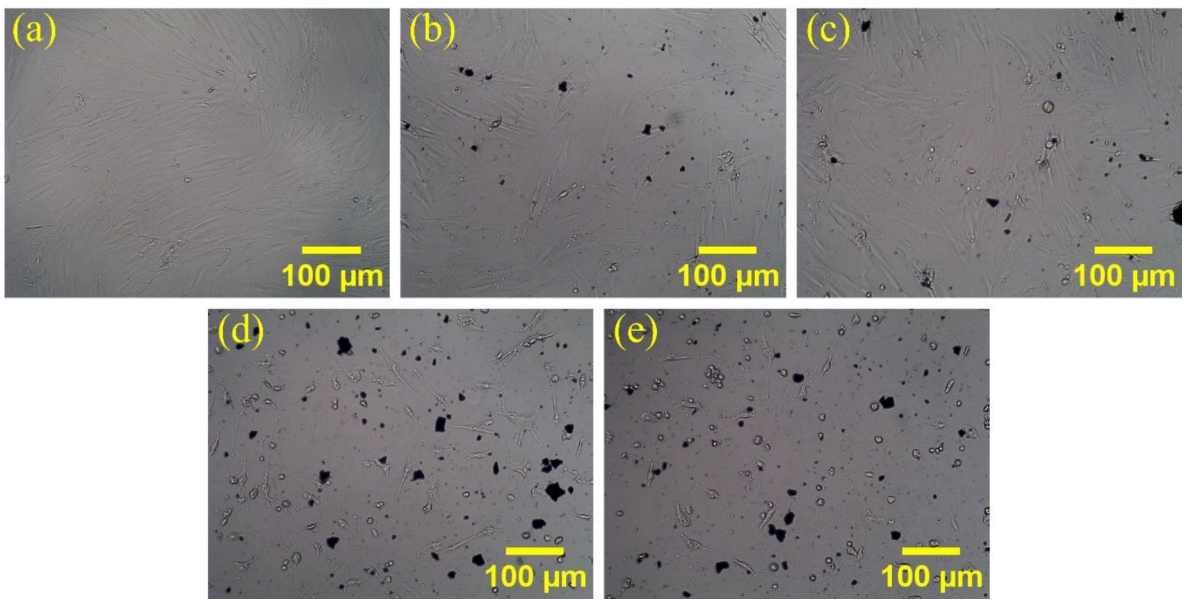

Fig. 8 Morphology of Human Dental Pulp Fibroblast cell in different concentrations. **A** Untreated (**B**, **C**, **D**, and **E**) (20, 30, 40, and 50 µM/ml) respectively

Conclusion

In conclusion, this work synthesizes tantalum and brass nanoparticles utilizing the µ-WEDG process, with variations in voltage and capacitance settings. The experimentation involves a range of capacitance values, specifically 400nF, 100nF, 10nF, and 1000pF, coupled with voltages of 120V, 110V, 100V, and 90V. The resulting nanoparticles are subjected to thorough characterization, leading to the following key findings and conclusions:

1) This study successfully synthesized tantalum and brass nanoparticles characterized by a spherical structure, utilizing the innovative µ-WEDG process.

The process yielded nanoparticles, the formation of which was notably influenced by capacitance. As capacitance values decreased, a concurrent reduction in nanoparticle size was observed. Nonetheless, it is imperative to underscore that further comprehensive investigations are essential to achieve precise control over particle Morphology.

2) The tantalum nanoparticles' typical crystal size was 25–200 nm, while the brass nanoparticles resided in the range of 300–950 nm, corresponding to a capacitance variation spanning 3–6. It is important to emphasize that extensive further investigations and experimentation are imperative to facilitate the mass production of nanoparticles using this innovative process.
3) Through comprehensive analysis employing FE-SEM, XRD, and EDX techniques, we successfully elucidated the produced nanoparticles' shape, size, and bonding characteristics. These findings provide valuable insights for envisaging prospective applications and avenues for utilizing these nanoparticles in future research and development.
4) Ta-Cu-Zn nanoparticles exhibit concentration-dependent cytotoxicity on Human Dental Pulp Fibroblast cells. Further in vivo and biocompatibility assessments are essential for the definitive safety evaluation of these nanoparticles for dental applications.

Acknowledgements
I want to express my appreciation to CRF NITK for generously providing the necessary facilities that enabled the successful execution of our experiments.

Patent
Application number: 20244103627, status: Published, Filing date: 07-05-2024, Title: Synthesis of Spherical Hybrid Nanoparticle using Non-traditional Micro Grinding (NTMG) Technique.

Author contributions
A.K: Drafted the manuscript and designed the figures with the input from all authors, Contributed to the method and approach of research and writing of manuscript. N.K.P: Analysis of research and writing of manuscript. A.K.S: Supervision, Analysis of research and writing of manuscript. B.M.J: Writing–review & editing, Supervision.

Funding
Not applicable.

Availability of data and materials
No datasets were generated or analysed during the current study.

Declarations

Competing interests
The authors declare no competing interests.

Received: 11 July 2024 Accepted: 11 September 2024
Published online: 27 September 2024

References

1. Liu T, Leng Y, Li X (2003) Preparation and characteristics of Fe3Al nanoparticles by hydrogen plasma-metal reaction. Solid State Commun 125(7–8):391–394. https://doi.org/10.1016/S0038-1098(02)00831-1
2. Lue JT, Huang WC, Ma SK (1995) Spin-flip scattering for the electrical property of metallic-nanoparticle thin films. Phys Rev B 51(20):14570–14575. https://doi.org/10.1103/PhysRevB.51.14570
3. Kumar P, Singh PK, Kumar D, Prakash V, Hussain M, Das AK (2017) A novel application of micro-EDM process for the generation of nickel nanoparticles with different shapes. Mater Manuf Process 32(5):564–572. https://doi.org/10.1080/10426914.2016.1244832
4. Huang W, Lue J (1999) Spin-glass properties of metallic nanoparticles conducted by quantum size effects. Phys Rev B Condens Matter Mater Phys 59(1):69–72. https://doi.org/10.1103/PhysRevB.59.69
5. Zouli N, Hakami J, Rudayni HA, Khan S (2014) Technological applications. Adv Exp Med Biol 794:141–163. https://doi.org/10.1007/978-94-007-7429-2__6
6. Darwish MA, Abd-Elaziem W, Elsheikh A, Zayed AA (2024) Advancements in nanomaterials for nanosensors: a comprehensive review. Nanoscale Adv. https://doi.org/10.1039/d4na00214h
7. Cruz-Martínez H, García-Hilerio B, Montejo-Alvaro F, Gazga-Villalobos A, Rojas-Chávez H, Sánchez-Rodríguez EP (2024) Density functional theory-based approaches to improving hydrogen storage in graphene-based materials. Molecules 29(2):1–17. https://doi.org/10.3390/molecules29020436
8. Wang L, Wang L, Meng X, Xiao FS (2019) New strategies for the preparation of sinter-resistant metal-nanoparticle-based catalysts. Adv Mater 31(50):1–18. https://doi.org/10.1002/adma.201901905
9. Mitra S, Muralidhara A, Vasa NJ, Singaperumal M (2010) Investigation on particle generation by micro-electro discharge machining. Micromach Microfabr Process Technol XV. https://doi.org/10.1117/12.845709
10. Korgal A, Shettigar AK, Karanth PN, Prabhakar DAP (2024) Advances in micro electro discharge machining of biomaterials: a review on processes, industrial applications, and current challenges. Mach Sci Technol 28(2):215–265. https://doi.org/10.1080/10910344.2024.2311376
11. Sahu RK, Hiremath SS (2019) Role of stabilizers on agglomeration of debris during micro-electrical discharge machining. Mach Sci Technol 23(3):339–367. https://doi.org/10.1080/10910344.2018.1486417
12. Bhiradi I, Hiremath SS (2020) Energy efficient and cost effective method for generation of in-situ silver nanofluids: formation, morphology and thermal properties. Adv Powder Technol 31(9):4031–4044. https://doi.org/10.1016/j.apt.2020.08.010
13. Singh Yadav HN, Das AK, Das M (2023) Synthesis of tungsten carbide nanoparticles in different dielectric through **M**-EDM. Adv Mater Process Technol 9(1):275–283. https://doi.org/10.1080/2374068X.2022.2091189
14. Roushan A, Biswas S (2024) Emerging sustainable techniques in metal cutting to reduce the application of metalworking Fl Uids : a review. https://doi.org/10.1177/09544089241256591
15. Sheu DY (2010) Microelectrode tools manufacturing by hybrid circuits twin-wire electrodischarge grinding. Mater Manuf Process 25(10):1142–1147. https://doi.org/10.1080/10426914.2010.502951
16. Pathania A, Dhanda N, Verma R, Sun A-CA, Thakur P, Thakur A (2024) Review—metal oxide chemoresistive gas sensing mechanism, parameters, and applications. ECS Sensors Plus 3(1):013401. https://doi.org/10.1149/2754-2726/ad2152
17. Wang LK, Wang MS, White WF (2024) Centrifugation process siting, sizing, and applications. Lenox Institute Press, Trenton. https://doi.org/10.17613/t8n3-xc72

Publisher's Note